Ultrasonic investigation of ZnSe:V^{2+} and ZnSe:Mn^{2+}: Lattice softening and low-temperature relaxation in crystals with orbitally degenerate states

V. V. Gudkov,[1,*] A. T. Lonchakov,[1,†] V. I. Sokolov,[1,‡] I. V. Zhevstovskikh,[1,§] and V. T. Surikov[2,‖]
[1]*Institute for Metal Physics, Ural Department of the Russian Academy of Sciences, 620041 Ekaterinburg, Russia*
[2]*Institute of Chemistry of Solid State, Ural Department of the Russian Academy of Sciences, 620041 Ekaterinburg, Russia*
(Received 24 July 2007; revised manuscript received 10 March 2008; published 24 April 2008)

Temperature dependences of elastic moduli and ultrasonic attenuation were investigated in ZnSe:V^{2+} and ZnSe:Mn^{2+} crystals as functions of temperature in the interval of 1.4–100 K for frequencies of 52–270 MHz. A peak in the attenuation was found in ZnSe:V^{2+} below 4 K for fast shear and longitudinal waves propagating along the [110] crystallographic axis. We interpret it to be a manifestation of a relaxation process related to the Jahn–Teller effect in the 3*d* electron system of the impurity. Softening of the elastic moduli C_{44} and $C_\ell = (C_{11}+C_{12}+2C_{44})/2$ were observed below 40 K. Temperature dependences were deduced for relaxation time and relaxed and unrelaxed C_{44} and C_ℓ moduli. The temperature dependence of relaxation time shows that ZnSe:V^{2+} has potential barrier $V_0=5.6$ cm^{-1}. Softening of the C_{44} modulus indicates that the local distortions have a trigonal character. Neither attenuation anomalies nor softening of the elastic moduli was observed in ZnSe:Mn^{2+}, which has a singlet orbital ground state of the 3*d* impurity.

DOI: 10.1103/PhysRevB.77.155210 PACS number(s): 61.72.uj, 43.35.+d, 62.20.D−, 64.70.K−

I. INTRODUCTION

Possible applications in optoelectronic and spintronic devices have stimulated interest in studying various properties of semiconductors doped with transition metals (see the book by Kikoin and Fleurov[1] and references therein).

Information about the energy states of an impurity's 3*d* electrons is very important and should be the starting point for the interpretation of most of the observed physical phenomena in these crystals. If the impurity has symmetry-degenerate electronic states in a tetrahedral or octahedral surrounding, the energy of the crystal is lowered by means of local lattice distortions that lift the degeneracy of the states. This phenomenon is known as the Jahn–Teller effect. In transition metal compounds, the distortions lead to a structural transition, i.e., a cooperative Jahn–Teller effect. Dilute semiconductors may not exhibit a phase transition, but a tendency toward a transition can be observed in the form of a softening of a symmetry-dependent elastic modulus. One may find a description of the Jahn–Teller effect and a discussion of experimental results in a review by Sturge[2] and recently published books by Lüthi[3] and Bersuker.[4]

Conventional techniques used for studying the Jahn–Teller effect are measurements of electron paramagnetic resonance and optical spectra of absorption and luminescence (see, for example, papers[5–8] relating to II–VI:3*d* crystals).

The energies of the phonons generated in an ultrasonic experiment are too small to be applied to the investigation of excited electron states; they are studied with the techniques mentioned above. However, ultrasonic attenuation measurements[9] in Al_2O_3:Ni^{3+} and YAlG:Mn^{3+} crystals, along with the appropriate interpretation of the data, have led to a new method for investigating the low energy levels located near the ground state, which are formed when the degeneracy is lifted.

The authors introduced a procedure for extracting the temperature dependence of the relaxation time τ by using ultrasonic attenuation α measured as a function of temperature. Moreover, by fitting $\tau(T)$ to a model of the relaxation effect, it was possible to evaluate parameters of the 3*d* electron system such as potential barrier, deformation potential, the Jahn–Teller splitting of energy levels, etc.[2]

Additional information can be obtained with the help of measurements of the temperature dependence of the ultrasonic velocity v or the elastic modulus $C=\rho v^2$, where ρ is the density of the material. Local Jahn–Teller distortions of the lattice are the result of changes in certain forces acting between the surroundings and an anion when an impurity is substituted for it. The directions of the forces determine the character of the vibronic modes and local distortions.

In a zinc-blende crystal, the modes of interest are the ϵ or τ_2 modes. The distortions that affect these modes have tetragonal $(2\varepsilon_{zz}-\varepsilon_{xx}-\varepsilon_{yy})$ or trigonal $(\varepsilon_{xy},\varepsilon_{yz},\varepsilon_{zx})$ character, respectively. On a macroscopic level, changes in the local forces are manifested as changes in a symmetry-dependent elastic modulus $(C_{11}-C_{12})/2$ for the tetragonal distortions and C_{44} for the trigonal ones. A detailed discussion has been given for GaAs:Cu.[10] In other words, by measuring the temperature dependences of such *phenomenological variables* as elastic moduli, we can determine the character of the local distortions and the types of vibronic modes, i.e., investigate parameters defined *at the elementary cell level*.

In our earlier experiments, carried out on ZnSe:Ni^{2+} [$^3T_1(e^4t^5)$ ground state] and ZnSe:Cr^{2+} [$^5T_2(e^2t^2)$], we found that (i) the C_{44} modulus in ZnSe:Ni^{2+} and the $(C_{11}-C_{12})/2$ modulus in ZnSe:Cr^{2+} exhibited softening below 100 K,[11,12] (ii) an attenuation peak was observed for the softening modes, (iii) the anomalies, both in $\alpha(T)$ and $C(T)$, were due to the 3*d* impurity (they were not observed in an undoped ZnSe crystal[13]), and (iv) the temperature at which the attenuation peak occurred changed in accordance with the equation which describes attenuation arising from relaxation.[14]

We proposed that the relaxation and softening were due to the Jahn–Teller effect. In the framework of this proposal, the experimental results could be interpreted as the observation

of trigonal distortions (the τ_2 vibronic mode) in ZnSe:Ni^{2+} and tetragonal ones (the ϵ mode) in ZnSe:Cr^{2+}. This was an important information because the character of the distortions in ZnSe:Cr^{2+} was not clear from emission and absorption spectra and, therefore, both trigonal and tetragonal distortions were used for the interpretation of the spectra.[8] As for ZnSe:Ni^{2+}, we are not aware of papers on this subject.

Although our interpretation was noncontradictory, nevertheless, it was based on the hypothesis of a relaxation process in the Jahn–Teller system. Experimental verification requires data on other ZnSe:3*d* compounds, including crystals which have no orbitally degenerate states, i.e., in which the Jahn–Teller effect cannot exist.

The present paper contains the results of experiments carried out on ZnSe:Mn^{2+} and ZnSe:V^{2+}. Mn^{2+} has a singlet ground state $^6A_1(e^2t^3)$, whereas V^{2+} has a triply degenerate states, $^4T_1(e^2t^1)$.

II. EXPERIMENT

A. Experimental details

The specimens were cut from single crystals with dopant concentrations of either $n_V=5.6\times10^{18}$ cm^{-3} or $n_{Mn}=9.4\times10^{20}$ cm^{-3}. Concentration was measured by using the inductively coupled plasma-mass spectroscopy technique by means of a Spectromass 2000 apparatus (SpectroAnalytical Instruments, Germany). The specimens had the form of a parallelepiped with distances between the parallel faces of $\ell_V=4.76$ mm and $\ell_{Mn}=4.99$ mm.

Experiments were carried out with the use of a pulse apparatus operating as a variable-frequency bridge.[15] Ultrasonic waves were propagated along ⟨110⟩. We studied all of the normal modes: longitudinal, slow shear (polarized along ⟨110⟩), and fast shear (polarized along ⟨100⟩) waves. The phase velocities of these modes are determined by the following elastic moduli: $C_\ell=(C_{11}+C_{12}+2C_{44})/2$ for the longitudinal mode, $C_{st}=(C_{11}-C_{12})/2$ for the slow shear (or transverse) mode, and C_{44} for the fast shear mode.

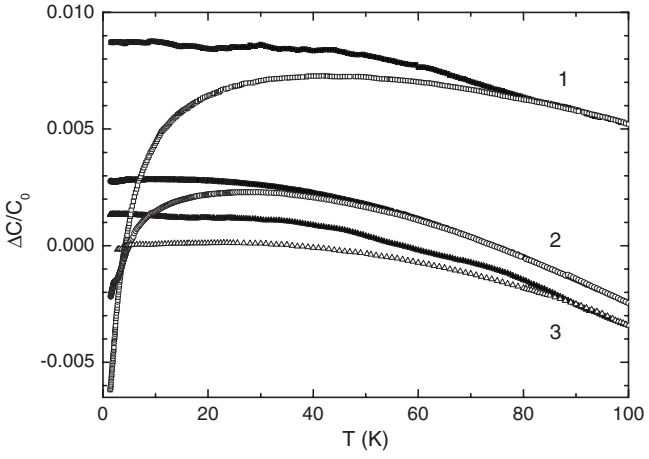

FIG. 1. Temperature dependences of the elastic moduli. Curve 1: $\Delta C_{44}(T)/C_{44}(T_0)$ (open circles—ZnSe:V^{2+}; filled—ZnSe:Mn^{2+}, frequency of 52 MHz for both plots); curve 2: $\Delta C_\ell(T)/C_\ell(T_0)$ (open circles—ZnSe:V^{2+}, 52 MHz; filled—ZnSe:Mn^{2+}, 55 MHz); and curve 3: $\Delta C_{st}(T)/C_{st}(T_0)$ (open circles—ZnSe:V^{2+}, 52 MHz; filled—ZnSe:Mn^{2+}, 55 MHz). $\Delta C_i(T)=C_i(T)-C_i(T_0)$, $T_0=4.2$ K. The plots for ZnSe:Mn^{2+} were shifted to coincide with the corresponding plots for ZnSe:V^{2+} at $T=100$ K.

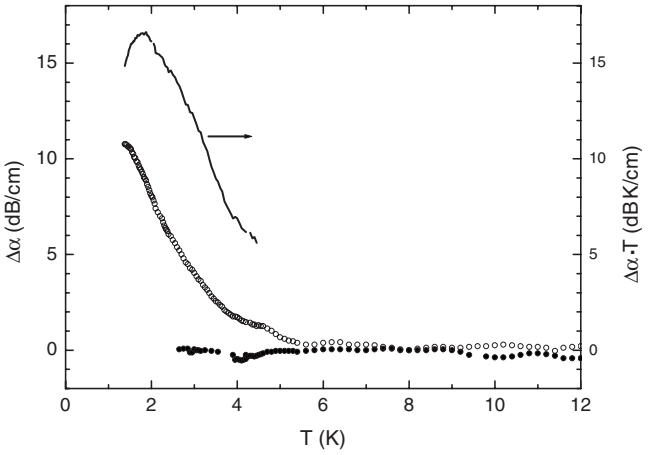

FIG. 2. Temperature dependences of ultrasonic attenuation for waves propagating in ZnSe:V^{2+} along the [110] axis: fast shear mode measured at 52 MHz (open circles) and slow shear mode measured at 55 MHz (filled circles). $\Delta\alpha=\alpha(T)-\alpha(T_0)$, $T_0=8$ K. The solid curve shows the dependence $\Delta\alpha(T)\cdot T$ for the fast shear mode at 52 MHz. Maximum of this curve corresponds to $\Delta\omega\tau=1$.

The ultrasonic waves were generated and detected by $LiNbO_3$ piezoelectric transducers in the 52–270 MHz frequency interval. The pulse duration τ_p was 0.7 μs. The accuracy of our measurements was $\approx$0.02 dB in attenuation and $\approx10^{-6}$ in $\Delta C/C_0$, where $\Delta C=C(T)-C(T_0)$ and T_0 is a reference temperature.

B. Dynamic moduli and ultrasonic attenuation

The temperature dependences of the dynamic (i.e., frequency-dependent) elastic moduli are given in Fig. 1. The moduli of ZnSe:Mn^{2+} do not show softening and we did not find anomalies in the attenuation for this crystal. The curves are similar to those obtained in undoped zinc selenide.[13]

In the case of ZnSe:V^{2+}, one can see that the C_{44} modulus exhibits appreciable softening. The C_ℓ modulus also softens because it contains C_{44} as a summand. The C_{st} modulus does not show softening; therefore, the local distortions in ZnSe:V^{2+} should have a trigonal character.

As for attenuation in ZnSe:V^{2+}, the slow shear mode did not exhibit an anomaly, which is in contrast with the fast shear mode. Figure 2 shows an increase in α for the 52 MHz fast shear mode at low temperatures. The attenuation was so large that it was not possible to use higher frequencies to investigate this anomaly. The longitudinal wave had less attenuation and we managed to carry out experiments at 52, 156, and 270 MHz. (see Fig. 3 for the results).

III. MORE GENERAL METHOD FOR EXTRACTING RELAXATION TIME

Interpretation of the previously mentioned ultrasonic experiments[2,9,11,14] was done under the assumption that the

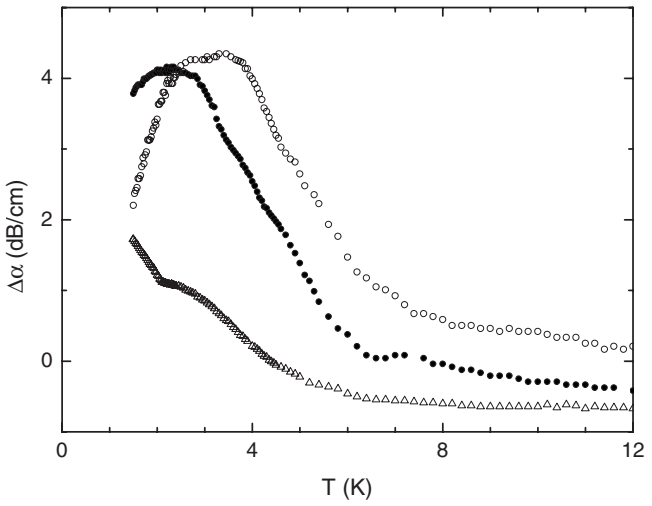

FIG. 3. Temperature dependences of ultrasonic attenuation for longitudinal waves propagating in ZnSe:V^{2+} along the [110] axis measured at 270 MHz (open circles), 156 MHz (filled circles), and 52 MHz (triangles). $\Delta\alpha=\alpha(T)-\alpha(T_0)$, $T_0=16$ K. The plot for 52 MHz is shifted downward by 0.7 dB for clarity.

attenuation had a relaxation origin and can be described (see, for example, Ref. 16) by

$$\alpha_r = \frac{k_0}{2}\frac{C^U - C^R}{C_0}\frac{\omega\tau}{1+(\omega\tau)^2}, \tag{1}$$

where ω is the radian frequency of the ultrasonic wave, $k_0=\omega/v_0$, $v_0=v(T_0)$, $C_0=\rho v_0^2$, and C^R and C^U are the relaxed and unrelaxed moduli, respectively. However, if a system contains at least two energy levels, resonant absorption may occur.[2,17] The equation for this kind of absorption is

$$\alpha_{res} = \frac{k_0}{2}\frac{C^U - C^R}{C_0}\frac{\omega\tau}{1+(\Delta\omega\tau)^2}, \tag{2}$$

where $\Delta\omega=\omega-\omega_0$ and $\hbar\omega_0$ is the energy separation of the ground and nearest excited states. In our case, the excited state is a result of tunneling splitting. One can see that the expression given in Eq. (1) represents the limit of the expression given in Eq. (2) corresponding to $\omega_0\to 0$ (i.e., $\omega \gg \omega_0$).

In the review cited earlier,[2] the parameter $(C^U-C^R)/C_0$ was assumed to be proportional to $1/T$. This dependence proved to be correct when several particular mechanisms of ultrasonic losses in semiconductors were considered.[16] We will also use this assumption in the present paper.

One may see that a maximum of resonant attenuation should be observed at $T=0$ for $\Delta\omega\tau\to 0$. If $\Delta\omega\tau\neq 0$ and ω_0 is a temperature-independent parameter, the function,

$$f_1(\omega\tau,\Delta\omega\tau) = \frac{\omega\tau}{1+(\Delta\omega\tau)^2}, \tag{3}$$

has a maximum at $|\Delta\omega|\tau=1$ but not at $\omega\tau=1$, as is the case for the function,

$$f_2(\omega\tau) = \frac{\omega\tau}{1+(\omega\tau)^2}, \tag{4}$$

which describes the relaxation attenuation given by Eq. (1). Note that if $|\omega-\omega_0|/\omega<1$, the peak of f_1 will be located at lower temperatures than that of f_2. If $|\omega-\omega_0|/\omega>1$, the peak will be observed at higher temperatures, but its magnitude will be appreciably reduced due to the small value of τ. Since the attenuation maximum in ZnSe:V^{2+} was observed at lower temperatures than in ZnSe:Ni^{2+} and ZnSe:Cr^{2+}, we will discuss its possible resonant origin.

It is easy to experimentally determine which of the frequencies, ω or ω_0, is smaller if τ is a monotonic function of T. Here, we will discuss the case of τ decreasing with temperature.

One can guess that if increasing ω leads to a shift of the attenuation peak to higher temperatures, the inequality $\omega>\omega_0$ holds true. Note that the same shift should occur for relaxation attenuation since it corresponds to an even stronger condition, $\omega\gg\omega_0$. If the peak is shifted to lower temperatures, the opposite inequality, $\omega<\omega_0$, should be realized. Figure 3 shows that a frequency increase leads to the shift of the peak to higher temperatures. Therefore, in our case, $\omega>\omega_0$ (or even $\omega\gg\omega_0$).

To generalize the method[2] for extracting the relaxation time, we should take into account both of the factors that shift the attenuation peak away from the temperature corresponding to $\omega\tau=1$: (i) temperature dependence of $(C^U-C^R)/C_0\propto 1/T$, which is important at low temperatures, and (ii) a finite value of ω_0.

We will discuss the experimental procedure consisting of measurements of $\alpha_{res}^{(1)}(T)$ and $\alpha_{res}^{(2)}(T)$ made with at least two fixed frequencies ω_1 and ω_2, respectively. By using Eq. (2), written the first time for an arbitrary temperature T and the second time for T_1, and assuming $\omega_1,\omega_2>\omega_0$, one can derive the following expressions:

$$(\omega_1-\omega_0)\tau(T) = F_1, \tag{5}$$

$$(\omega_2-\omega_0)\tau(T) = F_2, \tag{6}$$

where

$$F_i = \frac{\alpha_1^{(i)}T_1^{(i)}}{\alpha_{res}^{(i)}(T)T} \pm \sqrt{\left[\frac{\alpha_1^{(i)}T_1^{(i)}}{\alpha_{res}^{(i)}(T)T}\right]^2 - 1}. \tag{7}$$

In this expression, $i=1,2$, $T_1^{(i)}$ corresponds to $(\omega_i-\omega_0)\tau=1$, and $\alpha_1^{(i)}=\alpha_{res}^{(i)}(T_1^{(i)})$. Here, ω_0 is assumed to be a temperature-independent parameter or at least its temperature dependence should be sufficiently less pronounced than that of the relaxation time. For this case, measurements done in a certain temperature interval will give a statistical distribution characterizing their accuracy.

The system of Eqs. (5) and (6) can be solved with respect to ω_0 and τ to obtain

$$\omega_0 = \frac{\omega_1F_2-\omega_2F_1}{F_2-F_1}, \tag{8}$$

$$\tau(T) = \frac{F_2 - F_1}{(\omega_2 - \omega_1)}. \tag{9}$$

One important detail of the experiment should be mentioned here. Equation (2) describes resonant (or relaxation, if $\omega_0 \to 0$) attenuation. In our experiments, we measure total attenuation $\alpha(T)$. Therefore, the background attenuation $\alpha_b(T)$ should be subtracted from the measured values. In ZnSe:V^{2+}, the background attenuation at low temperatures was taken to be temperature independent. Thus, $\alpha_{res}^{(i)} = \Delta\alpha^{(i)} = \alpha^{(i)}(T) - \alpha^{(i)}(T_0)$. The magnitudes of T_0 can be found in the captions of Figs. 2 and 3.

The value of $\alpha_1^{(i)} T_1^{(i)}$ can be determined from the experimental data. If we multiply the left and right hand parts of Eq. (2) by T, the right hand part will represent the function $f_1(\omega\tau, \Delta\omega\tau)$ [see Eq. (3)] multiplied by a temperature-independent coefficient. Obviously, the product reaches its maximum value precisely at $(\omega - \omega_0)\tau = 1$. Note that this procedure for determining T_1 may be applied regardless of the attenuation type; it can be either resonant or relaxation. In the latter case, T_1 defines a maximum of $f_2(\omega\tau)$, given by Eq. (4), and corresponds to the condition $\omega\tau = 1$. Figure 3 shows that the positions of the attenuation peaks at 156 and 270 MHz were approximately 2 and 3 K, whereas the temperatures $T_1^{(i)}$, corresponding to $(\omega_i - \omega_0)\tau = 1$ and determined with the appropriate procedure, proved to be 3.55 and 3.95 K, respectively.

In some cases, this procedure can be applied even when the maximum of $\Delta\alpha(T)$ is located at such a low temperature that is not accessible in the experiment. For example, the lowest temperature we could reach was 1.4 K and we did not observe the attenuation maximum for the 52 MHz fast shear mode, but the temperatures corresponding to $(\omega - \omega_0)\tau = 1$, obtained with the use of the procedure described above, was 1.85 K (see Fig. 2). Thus, we were able to determine the relaxation time by using the data for longitudinal as well as fast shear modes at all the measurement frequencies.

Application of Eq. (8) to the data for ZnSe:V^{2+} with $\omega_1 = 270$ MHz and $\omega_2 = 52$ MHz resulted in a random distribution of ω_0 in the vicinity of zero (see Fig. 4). Thus, we can state that in our experiment, $\omega \gg \omega_0$, and we observe attenuation which has its origin in relaxation. It follows that we can use Eq. (5) with the assumption that $\omega_0 = 0$ and solve it for the relaxation time,

$$\tau = \frac{1}{\omega}\left[\frac{\alpha_1 T_1}{\alpha_r(T)T} \pm \sqrt{\left(\frac{\alpha_1 T_1}{\alpha_r(T)T}\right)^2 - 1}\right]. \tag{10}$$

This form of the expression differs from the one used in Ref. 2. We have replaced $\alpha_m T_m$ by $\alpha_1 T_1$, and T_1 is found as the temperature corresponding to the maximum of $\Delta\alpha(T) \cdot T$ but not of $\Delta\alpha(T)$. The difference is the result of taking into account the temperature dependence of $(C^U - C^R)/C_0$.

The relaxation time obtained with such a procedure is given in Fig. 5. It shows that $\tau(T)$ does not depend on either the frequency or the polarization of the wave. These features match completely what should be observed for relaxation in a Jahn–Teller system.

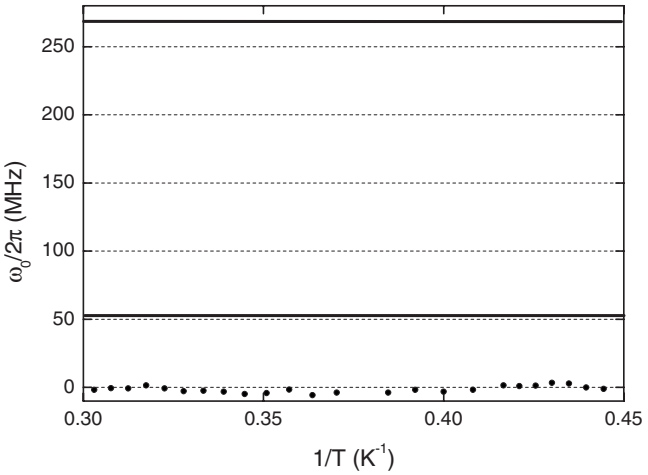

FIG. 4. The parameter $\omega_0/2\pi$ (open circles) plotted as a function of inverse temperature for a ZnSe:V^{2+} crystal, using data taken at 52 and 270 MHz. The solid lines show the highest (270 MHz) and the lowest (52 MHz) frequencies used in our experiment.

If one compares the relaxation time in ZnSe:V^{2+} (shown in Fig. 5), ZnSe:Cr^{2+} (Fig. 6, composed of data from Ref. 14), and ZnSe:Ni^{2+} (Fig. 7, the data taken from Ref. 11), one sees that all of the $\tau(T)$ curves are similar. Plotted logarithmically, they are represented by lines whose slopes change (indicated with arrows) at $1/T \approx 0.3$, 0.17, and 0.09 K^{-1}, respectively. The change of slope is interpreted[2] as a change in the relaxation mechanism: thermal activation over the potential barrier V_0 at higher temperatures and tunneling through the barrier at lower temperatures. The thermal activation mechanism is described by the relaxation rate,

$$\tau_T^{-1} = 2\nu_0 e^{-V_0/\kappa T} \equiv 2\nu_0 e^{-T_B/T}, \tag{11}$$

where κ is the Boltzmann constant and ν_0 is a constant with dimensions of frequency. The potential barrier can be

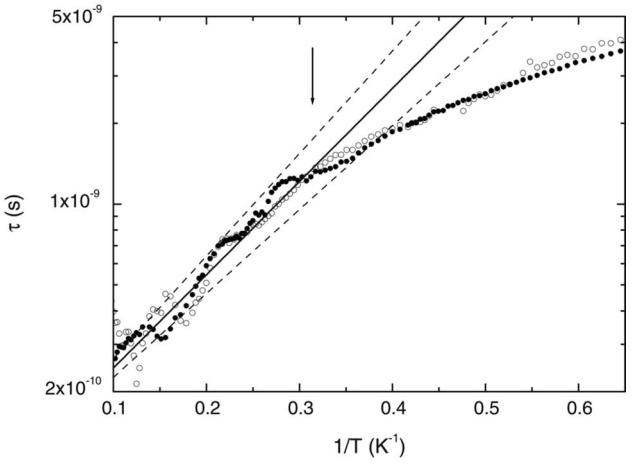

FIG. 5. Relaxation time versus inverse temperature in ZnSe:V^{2+}. The open circles show experimental data obtained with fast shear waves at 52 MHz; filled circles, with longitudinal waves at 156 MHz. The lines show $\tau = (2\nu_0)^{-1} e^{T_B/T}$. The solid line is for $T_B = 8$ K and the dashed line is for $T_B = 8 \pm 0.8$ K, $\nu_0 = 4.8 \times 10^9$ s^{-1}.

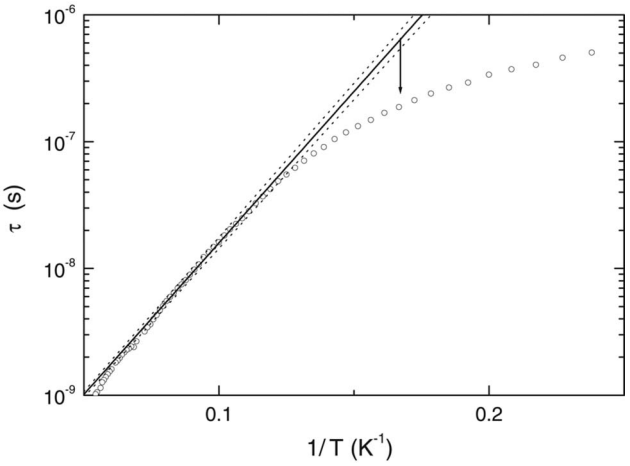

FIG. 6. Relaxation time versus inverse temperature in a ZnSe:Cr^{2+} crystal. The open circles show data obtained with longitudinal waves at 54.4 MHz. The lines are plots of $\tau=(2\nu_0)^{-1}e^{T_B/T}$; the solid line corresponds to $T_B=55$ K, and the dotted lines to $T_B=55\pm1$ K, $\nu_0=7.6\times10^9$ s^{-1}.

estimated from the slope of the high temperature part of the curve. For ZnSe:V^{2+}, we obtained $T_B=8.0\pm0.8$ K ($V_0=5.6\pm0.6$ cm^{-1}); for ZnSe:Cr^{2+}, $T_B=55\pm1$ K (38 ± 1 cm^{-1}); and for ZnSe:Ni^{2+}, $T_B=87\pm2$ K (60 ± 1 cm^{-1}).

IV. UNRELAXED AND RELAXED MODULI

Whenever data on $\tau(T)$ are obtained, one can use

$$\frac{C^U-C_0}{C_0}=2\left[\frac{\Delta v(T)}{v_0}+\frac{\alpha_r(T)}{k_0}\frac{1}{\omega\tau}\right] \tag{12}$$

and

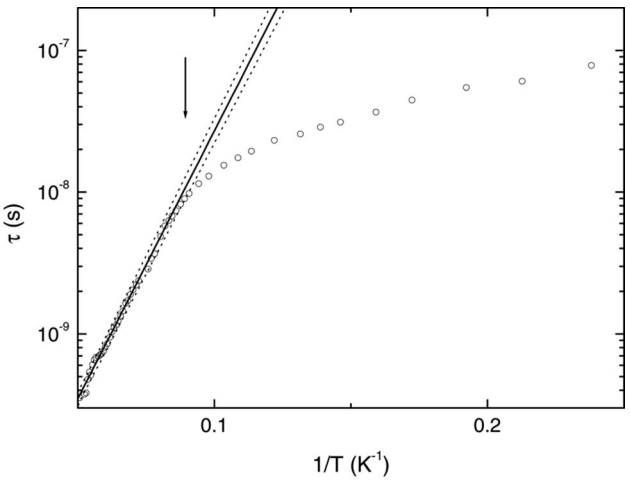

FIG. 7. Relaxation time versus inverse temperature in ZnSe:Ni^{2+}. The open circles show data obtained with fast shear waves at 56 MHz. The lines are plots of $\tau=(2\nu_0)^{-1}e^{T_B/T}$; the solid line corresponds to $T_B=87$ K, and the dotted lines to $T_B=87\pm2$ K, $\nu_0=11\times10^{10}$ s^{-1}.

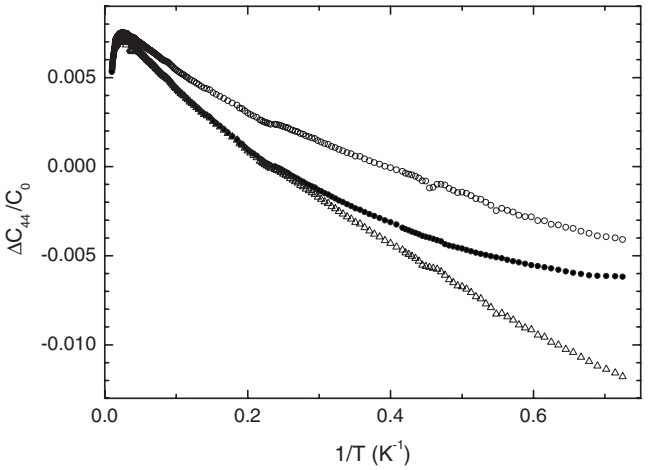

FIG. 8. Unrelaxed, relaxed, and dynamic moduli versus inverse temperature in ZnSe:V^{2+} measured at 52 MHz. $\Delta C_{44}^U/C_0$ (open circles), $\Delta C_{44}^R/C_0$ (triangles), and $\Delta C_{44}/C_0$ (filled circles). $\Delta C_{44}^i=C_{44}^i(T)-C_{44}(T_0)$, $C_0=C_{44}(T_0)$, $T_0=4.2$ K.

$$\frac{C^R-C_0}{C_0}=2\left[\frac{\Delta v(T)}{v_0}-\frac{\alpha_r(T)}{k_0}\omega\tau\right] \tag{13}$$

to determine the temperature dependences of the relaxed and unrelaxed moduli. These dependences for C_{44} and C_ℓ are given in Figs. 5 and 6, respectively. The principal features of the curves are similar to those observed in Ni^{2+} and Cr^{2+} doped ZnSe crystals: (i) there is a transformation of the dynamic modulus from a form close to relaxed at high temperatures to one close to unrelaxed at low temperatures, and (ii) the transformation takes place in the vicinity of $T=T_1$ (i.e., when $\omega\tau=1$). However, the transformation occurs at lower temperatures than in ZnSe:Ni^{2+} and ZnSe:Cr^{2+}. It is seen particularly well in Fig. 8 because the curves presented there are for the lowest frequency used in our experiments. Figure 9 shows a more complete transformation since the frequency

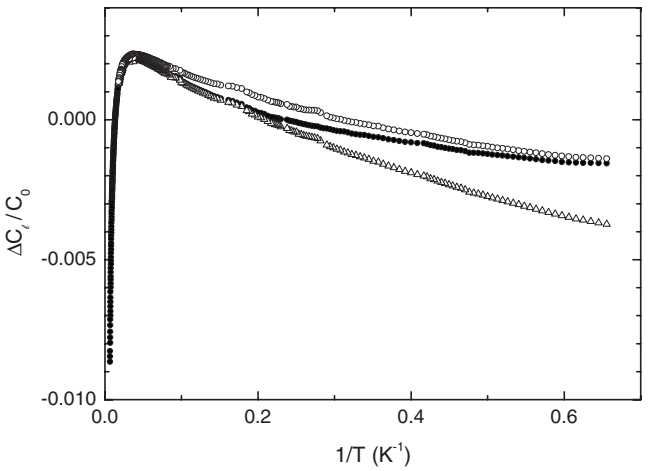

FIG. 9. Unrelaxed, relaxed, and dynamic moduli versus inverse temperature in ZnSe:V^{2+} measured at 156 MHz. $\Delta C_\ell^U/C_0$ (open circles), $\Delta C_\ell^R/C_0$ (triangles), and $\Delta C_\ell/C_0$ (filled circles). $\Delta C_\ell^i=C_\ell^i(T)-C_\ell(T_0)$, $C_0=C_\ell(T_0)$, $T_0=4.2$ K.

is higher and the condition $\omega\tau=1$ takes place at a higher temperature.

V. CONCLUSION

Investigations in a $ZnSe:Mn^{2+}$ crystal proved that the anomalies of relaxation attenuation and softening of a symmetry elastic modulus are not observed in a zinc-blende crystal with an orbital singlet ground state of the $3d$ impurity. This fact serves as a verification of the Jahn–Teller origin of the ultrasonic anomalies previously found in $ZnSe:Ni^{2+}$ and $ZnSe:Cr^{2+}$ at 13–19 K.

Anomalies in ultrasonic attenuation for the longitudinal and fast shear modes were found below 4 K in $ZnSe:V^{2+}$, as well as softening of the C_{44} modulus below 40 K. The softening of C_{44} provided evidence that the local distortions have a trigonal character in this crystal.

A procedure was developed for (i) estimating the energy separation $\hbar\omega_0$ of the ground and excited states and (ii) extracting the relaxation time for the case of resonant attenuation. In a $ZnSe:V^{2+}$ crystal, ω_0 proved to be much less than the lowest frequency used in our experiments, confirming the relaxation origin of the attenuation peak observed.

A generalization of the methods for extracting the temperature dependence of the relaxation time[2] in the case of relaxation attenuation was introduced and applied to a $ZnSe:V^{2+}$ crystal. The temperature dependence of the relaxation time showed that $ZnSe:V^{2+}$ has the potential barrier $V_0=5.6\ cm^{-1}$. Its value is lower than those previously found in $ZnSe:Cr^{2+}$ and $ZnSe:Ni^{2+}$ crystals. We also found the temperature dependences of frequency-independent relaxed and unrelaxed moduli.

ACKNOWLEDGMENTS

The authors appreciate the criticism and kind help of J. D. Gavenda and A. A. Demkov in the text preparation. This work was done within the Russian Academy of Sciences Program (Project No. 01.2.006 13395), with partial support from the Russian Foundation for Basic Research (Grant No. 04-02-96094-r2004 ural_a).

*Also at Ural State Technical University, Ekaterinburg, Russia. gudkov@imp.uran.ru
†lonchakov@imp.uran.ru
‡visokolov@imp.uran.ru
§zhevstovskikh@imp.uran.ru
‖surikov@icss.uran.ru

[1] K. A. Kikoin and V. N. Fleurov, *Transition Metal Impurities in Semiconductors: Electronic Structure and Physical Properties* (World Scientific, Singapore, 1994).
[2] M. D. Sturge, *Solid State Physics* (Academic, New York, 1967), Chap. The Jahn-Teller Effect in Solids, pp. 92–211.
[3] B. Luthi, *Physical Acoustics in the Solid State* (Springer, Berlin, 2004).
[4] I. B. Bersuker, *The Jahn-Teller Effect* (Cambridge University Press, Cambridge, 2006).
[5] H. J. von Bardeleben, C. Miesner, J. Monge, B. Briat, J. C. Launay, and X. Launay, Semicond. Sci. Technol. **11**, 58 (1996).
[6] O. Mualin, E. E. Vogel, M. A. de Orue, L. Martinelli, G. Bevilacqua, and H.-J. Schulz, Phys. Rev. B **65**, 035211 (2001).
[7] G. Bevilacqua, L. Martinelli, and E. E. Vogel, Phys. Rev. B **66**, 155338 (2002).
[8] G. Bevilacqua, L. Martinelli, E. E. Vogel, and O. Mualin, Phys. Rev. B **70**, 075206 (2004).
[9] E. M. Gyorgy, M. D. Sturge, D. B. Fraser, and R. C. LeCraw, Phys. Rev. Lett. **15**, 19 (1965).
[10] N. S. Averkiev, T. K. Ashirov, A. A. Gutkin, E. B. Osipov, and V. E. Sedov, Sov. Phys. Solid State **28**, 2961 (1986).
[11] V. Gudkov, A. Lonchakov, V. Sokolov, I. Zhevstovskikh, and N. Gruzdev, Phys. Status Solidi B **242**, R30 (2005).
[12] V. V. Gudkov, A. T. Lonchakov, V. I. Sokolov, and I. V. Zhevstovskikh, Low Temp. Phys. **33**, 269 (2007).
[13] V. V. Gudkov, A. T. Lonchakov, A. V. Tkach, I. V. Zhevstovskikh, V. I. Sokolov, and N. B. Gruzdev, J. Electron. Mater. **33**, 815 (2004).
[14] V. V. Gudkov, A. T. Lonchakov, V. I. Sokolov, and I. V. Zhevstovskikh, Phys. Rev. B **73**, 035213 (2006).
[15] V. V. Gudkov and J. D. Gavenda, *Magnetoacoustic Polarization Phenomena in Solids* (Springer-Verlag, New York, 2000), Chap. 3, pp. 25–31.
[16] M. Pomerantz, Proc. IEEE **53**, 1438 (1965).
[17] I. B. Bersuker, Sov. Phys. JETP **44**, 1577 (1963).